AMES-HET 99-03
UCRHEP-T251
BNL-HET-99/11

Graviton Production By Two Photon Processes In Kaluza-Klein Theories With Large Extra Dimensions

David Atwood[1]
Department of Physics and Astronomy, Iowa State University, Ames, IA 50011

Shaouly Bar-Shalom[2]
Department of Physics, University of California, Riverside, CA 92521

and

Amarjit Soni[3]
Theory Group, Brookhaven National Laboratory, Upton, NY 11973

Abstract:

We consider the production of gravitons via two photon fusion in Kaluza-Klein theories which allow TeV scale gravitational interactions. We find that the processes $\ell^+\ell^- \to \ell^+\ell^- + graviton$, with $\ell = e$, μ can put quite stringent bounds on such theories. For example, with two extra dimensions at the Next Linear Collider with a center of mass energy of 500 (1000) GeV attainable bounds on the scale of the gravitational interactions can reach about 6 (9) TeV.

[1]email: atwood@iastate.edu
[2]email: shaouly@phyun0.ucr.edu
[3]email: soni@bnl.gov

Gravity is the weakest force of nature and, although it ultimately controls the shape of the entire universe, its role in fundamental interactions remains obscure. This is due to the fact that gravity remains weak until the unreachably high scale of the Planck mass and thus there is no experimental data to construct a theory of gravity at small distances.

Of course the lack of experimental evidence has not deterred the construction of theories to account for the properties of gravitation at short distances. In this Letter we will consider certain Kaluza-Klein theories which contain additional compact dimensions besides the four space-time dimensions.

In such theories it was traditionally assumed that the compact dimensions form a manifold which is unobservably small (perhaps at the Planck scale) and thus remain hidden. However, recent advances in M-theory [1], a Kaluza-Klein theory in which there are 11 total dimensions suggest another possible scenario [2]. In models proposed in [2, 3], δ of these extra dimensions may be relatively large while the remaining dimensions are small. In this class of theories, the known fermions, the strong, weak and electromagnetic forces exist on a 4-brane while gravity may act in $4+\delta$ dimensions. The size of these extra dimensions, R, is related to an effective Planck mass, M_D, according to [2]:

$$8\pi R^\delta M_D^{2+\delta} \sim M_P^2 \tag{1}$$

where $M_P = 1/\sqrt{G_N}$ is the Planck mass and G_N is Newton's constant. Indeed the effective Planck mass at which gravitational effects become important may be as small as $O(1\ TeV)$ in which case such effects may be probed in collider experiments.

In this scenario, at distances $d < R$ the Newtonian inverse square law will fail [2]. If $\delta = 1$ and M_D=1 TeV, then R is of the order of 10^8 km, large on the scale of the solar system, which is clearly ruled out by astronomical observations. However, if $\delta \geq 2$ then $R < 1\ mm$; there are no experimental constraints on the behavior of gravitation at such scales [5] so these models are possible.

Astonishingly enough if $M_D \sim 1\ TeV$ then gravitons may be readily produced in accelerator experiments. This is because the extra dimensions give an increased phase space for graviton radiation. Another way of looking at this situation is to interpret gravitons which move parallel to the 4 dimensions of space time as the usual gravitons giving rise to Newtonian gravity while the gravitons with momentum components perpendicular to the brane are effectively a continuum of massive objects. The density of gravitons states is given by [2, 3, 6, 7]:

$$D(m^2) = \frac{dN}{dm^2} = \frac{1}{2} S_{\delta-1} \frac{\bar{M}_P^2 m^{\delta-2}}{M_D^{\delta+2}} \tag{2}$$

where m is the mass of the graviton, $\bar{M}_P = M_P/\sqrt{8\pi}$ and $S_k = 2\pi^{(k+1)/2}/\Gamma[(k+1)/2]$. The probability of graviton emission may thus become large when the sum over the huge number of graviton modes is considered.

Gravitons with polarizations that lie entirely within the physical dimensions are effective spin 2 objects which we consider in this Letter. Gravitons with polarizations partially or completely perpendicular to the physical brane are vector and scalar objects which we will not consider here since they couple more weakly than the spin 2 type.

The compelling idea that gravity may interact strongly at TeV scale energies has recently led to a lot of phenomenological activity. TeV scale gravity can be manifested either directly through real graviton production, leading to a missing energy signal, or indirectly through virtual graviton exchanges. Thus, existing and future high energy colliders can place bounds on the scale and the number of extra dimensions in these theories by looking for such signals [4], [6] – [15].

Typically, direct signals drop as $(E/M_D)^{\delta+2}$, where E is the maximum energy carried by the emitted gravitons. Therefore, the best limits on M_D from the existing experimental data at LEPII, Tevatron and HERA are obtained for the case $\delta = 2$. For example, existing LEPII data on $\sigma(e^+e^- \to \gamma + missing\ energy)$ already places the bound, $M_D \gtrsim 1\ TeV$ for $\delta = 2$ via the process $e^+e^- \to \gamma + G$ (see references [4, 6, 14]). For $\delta = 4$ the limit is $M_D \gtrsim 700$ GeV. A NLC with c.m. energy $\gtrsim 1\ TeV$ can push this limit up to $M_D \gtrsim 6\ TeV$ (for $\delta = 2$) and $M_D \gtrsim 4\ TeV$ (for $\delta = 4$) [4]. In hadronic colliders, the signal $p\bar{p} \to jet + missing\ energy$ can proceed by the subprocesses $q\bar{q} \to gG$, $q(\bar{q})g \to q(\bar{q})G$ and $gg \to gG$. Using these, the existing Tevatron data on $\sigma(p\bar{p} \to jet + missing\ energy)$ places the limits $M_D \gtrsim 750$ GeV for $\delta = 2$ and $M_D \gtrsim 600$ GeV for $\delta = 4$, while the LHC will be able to probe M_D up to $\sim 7\ TeV$ for $\delta = 2$ [4, 6].

The present bounds obtained from indirect signals associated with virtual graviton exchanges are typically $M_D \gtrsim 500 - 700$ GeV via processes such as $e^+e^- \to \gamma\gamma,\ ZZ,\ W^+W^-$ (LEPII) [13], $e^+q \to e^+q$ or $e^+g \to e^+g$ (HERA) [11, 12], $p\bar{p} \to t\bar{t} + X$ (Tevatron) [10], and $M_D \gtrsim 1\ TeV$ via processes such as $q\bar{q}, gg \to \ell^+\ell^-$ (Tevatron) and $e^+e^- \to f\bar{f}$ (LEPII) [9, 12]. Future colliders such as the NLC and the LHC will be able to push these limits to several TeV's through the study of these signals. Clearly other new physics can also give rise to similar signals so they may be used to bound TeV scale gravitation theories but can only confirm them with more extensive analysis, for example by angular distributions of final state particles (e.g. [9]). It should also be noted that the predictions in virtual graviton processes have some uncertainties since they depend on the sum over the Kaluza Klein (KK) tower of the massive excitations which is not fully determined without knowing the full quantum gravity theory.

In this paper we investigate another possible direct signal of strongly coupled low energy gravity via the process $e^+e^- \to e^+e^-G$ (G=spin 2 graviton) which proceeds predominantly through the t-channel $\gamma\gamma$ (or ZZ) fusion subprocesses $\gamma\gamma(ZZ) \to G$. Since these photons tend to be collinear, the process $e^+e^- \to e^+e^-G$ is significantly enhanced compared to s-channel processes. We find that the resulting signal is robust and possibly more useful for detecting or constraining some low energy gravity scenarios at the energy scales of a future NLC.

Let us now consider the excitation of spin 2 graviton modes through photon-photon and ZZ fusion. Such a process could be probed at an e^+e^- collider where the effective photon luminosity is generated by collinear photon emission. The complete process is therefore $e^+e^- \to e^+e^-G$ through the diagram shown in Fig. 1. In principle the other diagrams where the graviton is attached to the fermion lines or directly to the gauge-fermion vertex will also contribute, but the process in Fig. 1 should be dominant due to the enhancement of collinear gauge boson emission.

Let us consider first the case of photon-photon fusion. The cross section of this process may be estimated through the Weiszacker-Williams leading log approximation [16]. Thus if $\sum |\mathcal{M}(\hat{s})|^2$ is the matrix element for $\gamma\gamma \to G$, where G is a graviton of mass $m = \sqrt{\hat{s}}$, then in this approximation the total cross section for $e^+e^- \to e^+e^-G$ is given by:

$$\sigma(e^+e^- \to e^+e^-G) = \frac{\pi\eta^2}{4s}\int_0^1 \frac{f(\omega)}{\omega} D(\omega s)\sum|\mathcal{M}(\omega s)|^2 d\omega \qquad (3)$$

where s is the center of mass energy of the collision,

$f(\omega) = \left[(2+\omega)^2\log(1/\omega) - 2(1-\omega)(3+\omega)\right]/\omega$ and $\eta = \alpha\log\left[s/(4m_e^2)\right]/(2\pi)$.

Using the effective Lagrangian for the $G\gamma\gamma$ coupling derived in [6, 7], we obtain:

$$\sum|\mathcal{M}(\hat{s})|^2 = 2\frac{\hat{s}^2}{\bar{M}_P^2} \qquad (4)$$

Note that the explicit dependence on $\bar{M}_P$ will cancel when multiplied by the density of graviton states. This is typical of reactions involving real graviton emission. We therefore obtain the total cross section in this approximation:

$$\sigma_{\gamma\gamma}(e^+e^- \to e^+e^-G) = \frac{\alpha^2}{16\pi s} S_{\delta-1}\left[\frac{\sqrt{s}}{M_D}\right]^{\delta+2} F_{\frac{\delta}{2}} \log^2\left[\frac{s}{4m_e^2}\right] \qquad (5)$$

where $F_k = \int_0^1 f(\omega)\omega^k d\omega$.

In Fig. 2, the solid curves give the total cross section as a function of s given $M_D = 1\ TeV$ for $e^+e^- \to e^+e^-G$ in the cases where δ =2 and 6 (corresponding to the upper and lower solid curves) while the thin dashed curve is the cross section for $\mu^+\mu^- \to \mu^+\mu^-G$ with $\delta = 2$ which would be applicable to a muon collider.

Experimental considerations suggest that perhaps the full cross section which is given in the above is not observable. Gravitons couple very weakly to normal matter and thus a radiated graviton will not be detected in the detector. Therefore, the signature for the reaction would be

$$e^+e^- \to e^+e^- \ + \ missing\ mass.$$

Since this cross section is dominated by emission of photons at a small angle, the outgoing electrons will therefore also be deflected by a small angle.

Although one can expect that the electrons will suffer an energy loss, a significant portion of the electrons will not be deflected out of the area of the beam pipe and so may not be directly detected. To obtain a more realistic estimate one must therefore select events where the electron is deflected enough to be detected. Moreover, there is a Standard Model background to this signal from the process $e^+e^- \to e^+e^-\nu_\ell\bar{\nu}_\ell$. The component of this cross section which results from ZZ fusion, $ZZ \to \nu_\ell\bar{\nu}_\ell$, in particular, has a P_T distribution similar to the signals we consider. We calculate this background using the effective boson approximation [17]. This background is 0.25 fb for $\sqrt{s} = 500\ GeV$ and 1.6 fb at $\sqrt{s} = 1\ TeV$. Let us now consider three possible methods for detection of this signal.

First, one could take advantage of the fact that a significant amount of energy present in the initial collision is lost to the unobservable graviton. In Fig. 3, the normalized missing mass distribution is shown as a function of $\omega = \hat{s}/s$ where $\hat{s}$ is the missing mass squared of the graviton. In this approximation, this distribution is not changed by the value of $\sqrt{s}$, M_D or any systematic cut imposed on the transverse momentum P_T of the outgoing electrons. The distribution is shown for $\delta = 2$ (solid), $\delta = 4$ (dashed), $\delta = 6$ (dotted) and $\delta = 8$ (dot-dash). In principle it might be possible to separate the reduced energy electrons form the outgoing electrons of the collision at a e^+e^- collider through downstream dipole magnets but the large bremsstrahlung radiation generated by the disruption of the collision probably makes such an electron difficult or impossible to detect. At a muon collider, perhaps a Roman Pot could find reduced energy muons which were deflected from the main beam however the decay electrons in the muon collider environment may make this difficult also. Clearly experimental innovations are required to detect the full cross section and we will not consider this further.

Secondly, if both of the electrons are given enough of a transverse momentum that they may be detected in the detector or the end-caps, events of the desired type may be identified. Using the leading log approximation, one can use Eqn. 3 with η replaced by $\hat{\eta}(P_{Tmin}) = \alpha \log\left[s/(4P_{Tmin})\right]/(2\pi)$ where P_{Tmin} is the minimum transverse momentum of the outgoing electron which is accepted. If one imposes this cut on the two outgoing electrons one obtains the cross section as a function of $\hat{s}$ shown in Fig. 2 with the dotted curve for the case of $P_{Tmin} = 10$ GeV with $M_D = 1\ TeV$ and $\delta = 2$, while the heavy dot-dot-dash curve is for $\delta = 4$. These curves would be the same at both electron and muon colliders since the transverse momentum cut is well above the lepton mass. The missing mass spectra under this cut should also correspond to the curves shown in Fig. 3.

The missing mass spectrum for the background discussed above is shown in the case of $\sqrt{s} = 1\ TeV$ with the dot-dot-dash line (The normalization of this curve is reduced by 1/10 for clairity). Clearly this distribution differs markedly from the signal and cuts may thus be used to enhance the discrimination between signal and background. To obtain bound on M_D we will consider a cut of $\omega > 0.16$ which reduces the background to 0.19 fb. In contrast, the signal is reduced by a factor of 0.42 in the case of $\delta = 2$, 0.82 in the case of $\delta = 4$, 0.96 in the case of $\delta = 6$ and 0.99 in the case of $\delta = 8$.

Thirdly, one could identify events where only one of the electrons has a transverse momentum greater than P_{Tmin}. This would in effect be replacing η^2 in Eqn. 3 with $\eta_{eff}^2 = 2\eta(\eta - \eta(P_{Tmin}))$. The resultant cross sections are shown in Fig. 2 with the dot-dash curve for $P_{Tmin} = 20$ Gev. In this case, the energy of the detected electron will be markedly reduced from the beam energy since the graviton mass distribution increases at high masses. In Fig. 4 we show the normalized missing energy (E_{miss}) spectrum as a function of $x = 2E_{miss}/\sqrt{s} = E_{miss}/E_{beam}$ for the detected electron where $\delta = 2$ (solid), $\delta = 4$ (dashed), $\delta = 6$ (dotted) and $\delta = 8$ (dot-dash). In this leading log approximation, the curves of Fig. 4 are largely independent of P_{Tmin}.

The missing energy spectrum for the background is shown in the case of $\sqrt{s} = 1\ TeV$ with the dot-dot-dash line (with 1/2 the normalization). Again a cut in x can enhance the the signal with respect to the background somewhat. If we impose the cut $x > 0.2$, the background is reduced to 0.78 fb, while the signal is reduced by a factor of 0.72 in the case of $\delta = 2$, 0.93 in the case of $\delta = 4$, 0.99 in the case of $\delta = 6$ and 0.997 in the case of $\delta = 8$.

Let us now consider the related process $e^+e^- \rightarrow ZZe^+e^- \rightarrow e^+e^-G$ which can likewise be estimated by the effective vector boson leading log approximation. In general the cross section is given by a sum over cross sections for $ZZ \rightarrow G$ in various helicity combinations together with the helicity dependent structure functions given in [17]. Here there is considerable simplification since in this approximation where the boson momenta are taken collinear with their parent leptons, the only amplitude which contributes are the cases where the bosons are transverse and of opposite helicities. As with the photon, we use the effective Lagrangian from [6] and obtain the cross section in this approximation:

$$\sigma_{ZZ}(e^+e^- \to e^+e^-G) = \frac{y^2\alpha^2}{16\pi s} S_{\delta-1} \left(\frac{\sqrt{s}}{M_D}\right)^{\delta+2} \left[F^Z_{\frac{\delta}{2}}(s) + z^2 H^Z_{\frac{\delta}{2}}(s)\right] \log^2\left(\frac{s}{M_Z^2}\right) \quad (6)$$

where

$$\begin{aligned}
&x_w = \sin^2\theta_w, \qquad y = \frac{1-4x_w+8x_w^2}{8x_w(1-x_w)}, \qquad z = \frac{1-4x_w}{2(1-4x_w+8x_w^2)}, \\
&F^Z_k(s) = \int_{\frac{4m_Z^2}{s}}^1 \omega^k f(\omega) d\omega \\
&H^Z_k(s) = -\int_{\frac{4m_Z^2}{s}}^1 4\omega^k \left[(4+\omega)log(\frac{1}{\omega}) - 4(1-\omega)\right] \qquad (7)
\end{aligned}$$

and $f(\omega)$ is defined as for the case of photons.

In Fig. 2 the thick dashed curve shows the total cross section for this process given $M_D = 1\ TeV$ and $\delta = 2$. This cross section is flat in P_T for $P_T < O(m_Z)$ and therefore $O(10\ GeV)$ cuts in P_T of the outgoing leptons will not reduce this greatly. For the same reason the cross section at a $\mu\mu$ collider will be the same.

In Table 1 we consider the limits that may be placed on theories with extra dimensions using these $e^+e^- \to e^+e^-G$ processes. We consider three possible accelerator scenarios: $\sqrt{s} = 200\ GeV$ and a total integrated luminosity of $2.5\ fb^{-1}$ (for LEP-200); $\sqrt{s} = 500\ GeV$ and a total integrated luminosity of $50\ fb^{-1}$; $\sqrt{s} = 1\ TeV$ and a total integrated luminosity of $200\ fb^{-1}$. These last two cases correspond to a future NLC. For $\sqrt{s} = 1\ TeV$ we will impose the cut of $\omega > 0.16$ on both the signal and the background in the case where both electrons are subject to the $P_{Tmin} = 10\ GeV$ cut and a cut of $x > 0.2$ if only one electron is subjected to this cut. We define the lower limit on M_D in each case to be the value which will yield 10 events in each scenario or a signal of statistical significance of 3σ above the background. For $\delta = 2$, 4 and 6 we consider detection either via the full cross section (if that were somehow observable) or via the signal with the cut $P_{Tmin} = 10\ GeV$ on just one outgoing electron or both outgoing electrons.

As can be seen, using the two electron signal, at the 200 GeV collider, a limit of about 0.5-2 TeV (depending on δ) may be placed on M_D; using the 500 GeV collider a limit of about 1-6 TeV may be obtained and with a 1 TeV collider a limit of about 2.5-9 TeV may result. Clearly the limit on M_D decreases somewhat as δ increases. Obviously, with less stringent cuts and/or using a single high P_T lepton tag the lower limit on M_D may be increased somewhat.

If a signal is seen, the missing mass distributions in Fig. 3 and the missing energy distributions in Fig. 4 will help distinguish these theories from other new physics candidates and also help to determine how many extra dimensions are present.

We are grateful to Jose Wudka for discussions. One of us (DA) thanks the UCR Theory Group for hospitality. This research was supported in part by US DOE Contract Nos. DE-FG01-94ER40817 (ISU), DE-FG03-94ER40837 (UCR) and DE-AC02-98CH10886 (BNL)

Table 1

$\delta = 2$				
$\sqrt{s}$	$\int \mathcal{L} dt$	No cut	$P_{Tmin} = 10\ GeV$ (one electron)	$P_{Tmin} = 10\ GeV$ (two electrons)
200 GeV	2.5 fb^{-1}	2.4 TeV	1.8 TeV	1.0 TeV
500 GeV	50 fb^{-1}	8.2 TeV	6.4 TeV	4.4 TeV
1000 GeV	200 fb^{-1}	14.4 TeV	8.9 TeV	6.2 TeV
$\delta = 4$				
$\sqrt{s}$	$\int \mathcal{L} dt$	No Cut	$P_{Tmin} = 10\ GeV$ (one electron)	$P_{Tmin} = 10\ GeV$ (two electrons)
200 GeV	2.5 fb^{-1}	1.0 TeV	0.8 TeV	0.5 TeV
500 GeV	50 fb^{-1}	3.0 TeV	2.6 TeV	2.0 TeV
1000 GeV	200 fb^{-1}	5.4 TeV	4.1 TeV	3.5 TeV
$\delta = 6$				
$\sqrt{s}$	$\int \mathcal{L} dt$	No Cut	$P_{Tmin} = 10\ GeV$ (one electron)	$P_{Tmin} = 10\ GeV$ (two electrons)
200 GeV	2.5 fb^{-1}	0.6 TeV	0.5 TeV	0.4 TeV
500 GeV	50 fb^{-1}	1.8 TeV	1.6 TeV	1.3 TeV
1000 GeV	200 fb^{-1}	3.3 TeV	2.7 TeV	2.4 TeV

Table 1: The limits on the parameter M_D are given for $\delta = 2$, 4 and 6. In each case three accelerator scenarios are considered with $\sqrt{s} = 200\ GeV$, $500\ GeV$ and $1000\ GeV$ with luminosities 2.5 fb^{-1}, 50 fb^{-1} and 200 fb^{-1} respectively. The signals considered are based on the total cross section, the cross section with one electron passing the $P_{Tmin} = 10\ GeV$ cut and the cross section with both electrons passing the $P_{Tmin} = 10\ GeV$ cut. The limit which is placed on M_D is based on the criterion of 10 events for the given luminosity or a significance of 3σ above the background.

References

[1] P. Horava and E. Witten, Nucl. Phys. **B460**, 506 (1996); *ibid.* Nucl. Phys. **B475**, 94 (1996); E. Witten, Nucl. Phys. **471**, 135 (1996); I. Antoniadis, Phys. Lett. **B246**, 377 (1990); P. Ginsparg, Phys. Lett. **B197**, 139 (1987).

[2] N. Arkani-Hamed, S. Dimopoulos and G. Dvali, Phys. Lett. **B429**, 263 (1998); I. Antoniadis, N. Arkani-Hamed, S. Dimopoulos and G. Dvali, Phys. Lett. **B436**, 257 (1998).

[3] J. Lykken, Phys. Rev. **D54**, 3693 (1996); J. Dienes, E. Dudas and T. Ghergetta, Phys. Lett. **B436**, 55 (1998). G. Shiu and S.H. Tye, Phys. Rev. **D58**, 106007 (1998).

[4] E.A. Mirabelli, M. Perelstein and M.E. Peskin, Phys. Rev. Lett. **82**, 2236 (1999).

[5] V. P. Mitrofanov and O. I. Ponomareva, Sov. Phys. JETP **67**, 1963 (1988); J. C. Long, H. W. Chan and J. C. Price, Nucl. Phys. **B539**, 23 (1999) and references therein.

[6] G.F. Giudice, R. Rattazzi and J.D. Wells, Nucl. Phys. **B544**, 3 (1999).

[7] T. Han, J.D. Lykken and R. Zhang, hep-ph/9811350 (1998).

[8] S. Nussinov and R. Shrock, Phys. Rev. **D59**, 105002 (1999).

[9] J.L. Hewett, hep-ph/9811356 (1998).

[10] P. Mathews, S. Raychaudhuri and K. Sridhar, hep-ph/9811501 (1998).

[11] P. Mathews, S. Raychaudhuri and K. Sridhar, hep-ph/9812486 (1998).

[12] T.G. Rizzo, hep-ph/9901209 (1999).

[13] K. Agashe and N.G. Deshpande, hep-ph/9902263 (1999).

[14] K. Cheung and W. Keung, hep-ph/9903294 (1999).

[15] T. G. Rizzo, hep-ph/9903475 (1999).

[16] *see e.g.* M. Peskin and D. Schroeder. "An Introduction to Quantum Field Theory", p. 578, Addison-Wesley Publishing Company (1995).

[17] See e.g., S. Dawson, Nucl. Phys. **B249**, 42 (1985); P. W. Johnson, F. I. Olness and W. K. Tung, Phys. Rev. **D36**, 291 (1987); R.P. Kauffman, Phys. Rev. **D41**, 3343 (1990); V. D. Barger and R. J. N. Phillips, "Collider Physics", Addison-Wesley publishing company (1987).

Figure Captions

Figure 1: The dominant Feynman diagram for $e^+e^- \to e^+e^-G$ through an effective photon or Z sub-process.

Figure 2: The cross sections for various processes are shown as a function of $\sqrt{s}$. The solid lines are the total cross sections for $\delta = 2$ (upper curve) and $\delta = 6$ (lower curve). The dotted line is for the case that both the outgoing electrons are subject to the cut $P_{Tmin} = 10\ GeV$ and for $\delta = 2$. The dot-dash line is obtained again with $\delta = 2$ but now only one of the outgoing electrons is subject to the cut $P_{Tmin} = 20\ GeV$. The thick dot-dot-dash line is for $\delta = 4$ where both of the outgoing electrons are subject to the cut $P_{Tmin} = 10\ GeV$. The thick dashed line shows the total cross section for $\delta = 2$ via the ZZ process. The dashed line gives the cross section for $\mu^+\mu^- \to \mu^+\mu^-G$ for $\delta = 2$ via the $\gamma\gamma$ process. In all cases we take $M_D = 1\ TeV$.

Figure 3: The normalized differential cross section as a function of the scaled missing (graviton) invariant mass squared ($\omega = \hat{s}/s$) for $\delta = 2$ (solid line), $\delta = 4$ (dashed line), $\delta = 6$ (dotted line), $\delta = 8$ (dot-dash line). These curves are not greatly effected by the P_{Tmin} cut, M_D or s. The dot-dot-dash curve shows $(1/10)d\sigma/(\sigma d\omega)$ for the background.

Figure 4: The normalized differential cross section as a function of the missing energy of the single detected electron. See also caption to Fig. 3. Here, the dot-dot-dash curve shows $(1/2)d\sigma/(\sigma dx)$ for the background.

Figure 1

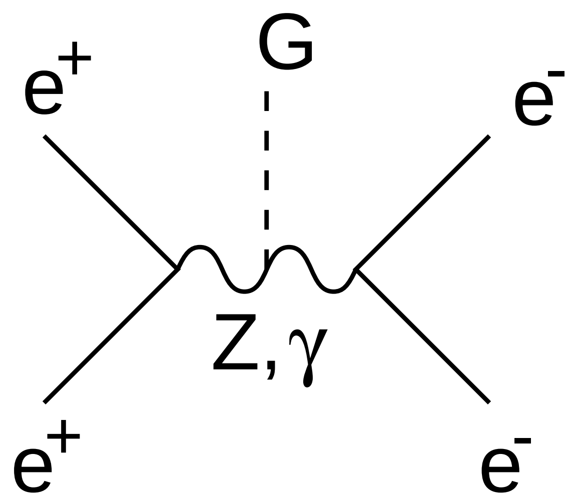

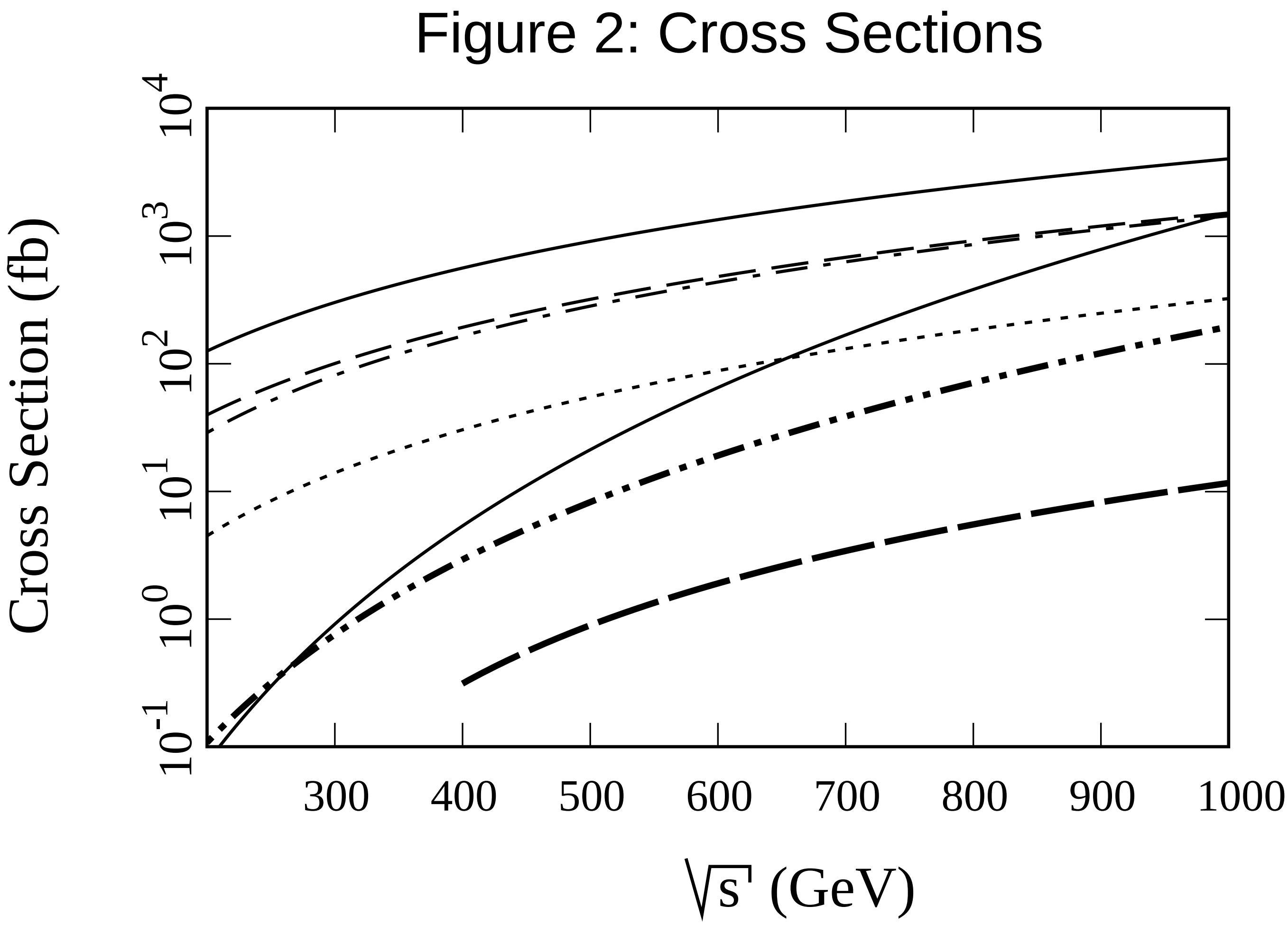

Figure 2: Cross Sections
Cross Section (fb)
10^4
10^3
10^2
10^1
10^0
10^-1
300
400
500
600
700
800
900
1000
√s' (GeV)

Figure 3: Missing Mass Distribution

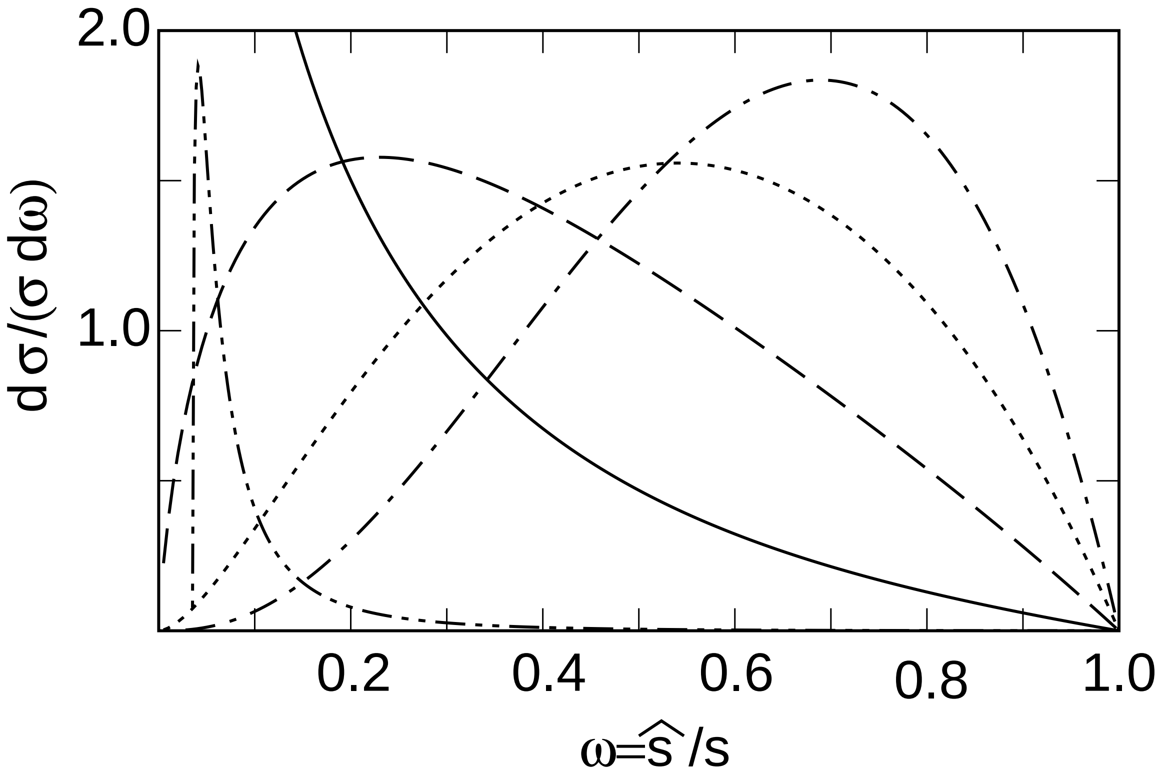

Figure 4: Single Lepton Missing Energy Distribution